

16-qubit IBM universal quantum computer can be fully entangled

Yuanhao Wang,¹ Ying Li,² Zhang-qi Yin,^{1,*} and Bei Zeng^{3,4}

¹Center for Quantum Information, Institute for Interdisciplinary Information Sciences, Tsinghua University, Beijing 100084, China

²Graduate School of China Academy of Engineering Physics, Beijing 100193, China

³Department of Mathematics and Statistics, University of Guelph, Guelph N1G 2W1, Ontario, Canada

⁴Institute for Quantum Computing and Department of Physics and Astronomy, University of Waterloo, Waterloo N2L 3G1, Ontario, Canada

Multipartite entanglement is an important evidence that a quantum device can potentially solve problems intractable for classical computers. In this paper, we report on genuine multipartite entanglement of up to 16 qubits on *ibmqx5*, a 16-qubit superconducting quantum processor accessible via IBM cloud. Connected graph states involving 8 to 16 qubits are prepared on *ibmqx5* using low-depth circuits. We demonstrate that any pair of qubits connected on the graph are entangled, therefore for any cut on the graph two parts are entangled, i.e. the entanglement is genuine. Our results set a new record for the number of genuinely entangled qubits for both superconducting circuits and trapped ions systems.

PACS numbers:

I. INTRODUCTION

Quantum computation has become an active research topic since middle 90s with the invention of the Shor's algorithm and many other important discoveries such as quantum error correction [1]. For the last two decades, physical implementations of quantum computation have achieved significant progress. The single and two-qubit gates fidelity reaches 99%, or more, for performing universal quantum computing. The number of qubits in both superconducting and trapped ions quantum computers becomes larger than 20 now [2, 3]. It is projected that the number of qubits will approach to 50 or more in the next few years. At that time, the quantum computer may become more powerful than the fastest classical computer for some specific tasks, into the regime of the so called quantum supremacy [4].

The IBM Q is a quantum cloud service released by IBM. Its present backend devices include two processors with 5 superconducting qubits (*ibmqx2* and *ibmqx4*), one 16 qubit processor (*ibmqx5*) and one 20 qubit processor (*Q51.1*) [3]. IBM recently announced that they have successfully built and tested a 20-qubit and a 50-qubit machine [3]. The quantum cloud service by IBM realized high fidelity quantum gate operations and measurements. Hence, after the launch of the IBM Q, many groups tested it and performed quantum computing experiments on the cloud; for instance, see [5–11].

Entanglement is considered to be the most nonclassical manifestation of quantum physics [12]. It is also a critical resource for quantum information processing. Highly entangled states such as Bell states, GHZ states and clus-

ter states [13] have been applied in quantum teleportation, super-dense coding, one-way quantum computing [14] and various quantum algorithms. Up to now, the largest number of genuinely entangled qubits reported for a superconducting quantum computing device is 10 [15]. The ability to produce highly-entangled states is, therefore, one important step to demonstrate quantumness for quantum processors like *ibmqx5*. This task is, however, highly non-trivial due to the error accumulation of faulty gates. For instance, recently in a fully controlled 20-qubit trapped ions system, the genuine multipartite entanglement can only be observed up to 5 qubits [2].

In this paper, we wish to assess the quantumness and performance of the 16 qubit *ibmqx5* device via the production of highly entangled states, namely the graph states, which is an important class of many-body entangled states that have widely used in one-way quantum computing, quantum error correction [14, 16]. We generate graph states that correspond to rings involving 8 to 16 qubits via the IBM Q cloud service (*ibmqx5*), using optimized low-depth circuits that are tailored to the universal gate set on *ibmqx5*. We detect genuine many-body entanglement up to 16 qubits, using an entanglement criterion based on reduced density matrices. In this way, we set a new record for the number of genuinely entangled superconducting qubits. Besides, our results also exceed the record in the trapped ions, where the largest number of genuine entangled qubits is 14 [17].

We organize our paper as follows. In Section II, we include some preliminary materials, especially the concept, construction process and properties of graph states, as well as the idea of entanglement criterion based on reduced density matrices; In Section III, we discuss the preparation of graph states on *ibmqx5* of 8, 10, 12, 14 and 16 qubits, by designing optimized low-depth gate circuits tailored to the universal gate set of the device; In Section IV we discuss the entanglement properties of the

*Electronic address: yinzhangqi@tsinghua.edu.cn

graphs states based on a criterion of reduced density matrices, by analyzing experimental data; A summary and discussion of future work is given in Section V.

II. GRAPH STATES AND ENTANGLEMENT

A. Graph states

Graph state [18] is a generalisation of cluster state introduced in 2001 [13], which is the resource state of one-way quantum computing [14] and quantum error correction [16]. GHZ state is an example of graph state and has been demonstrated in superconducting qubit system [15]. However, GHZ state is fragile. Some other graph states are very robust to local operations, such as local measurements and noises. In order to disentangle the cluster state of N qubits, $N/2$ local measurements are needed [13]. Because of this nice feature, we decide to generate and detect linear cluster states in the IBM cloud service *ibmqx5*.

X, Y, Z denote the Pauli operators. An undirected graph $G(V, E)$ includes a set of vertices V and a set of edges E . A graph state that correspond to an undirected graph $G(V, E)$ is a $|V\rangle$ -qubit state that has the form

$$|G\rangle = \prod_{(a,b) \in E} U_{ab} |+\rangle^{\otimes V}, \quad (1)$$

where U_{ab} is a control-Z operator acting on qubits a and b [19], and

$$|\pm\rangle = \frac{1}{\sqrt{2}}(|0\rangle \pm |1\rangle) \quad (2)$$

are eigenvectors of the X operator.

An equivalent definition is, the graph state that corresponds to $G(V, E)$ is the unique common eigenvector (of eigenvalue 1) of the set of independent commuting operators:

$$K_a = X^a Z^{N_a} = X^a \prod_{b \in N_a} Z^b, \quad (3)$$

where the eigenvalues to K_a are $+1$ for all $a \in V$, and N_a denotes the set of neighbor vertices of a in G [19]. As implied by the first definition, a n -qubit graph state can be prepared by the following steps.

1. Initialize the state to $|+\rangle^{\otimes n}$ by applying n Hadamard gates to $|0\rangle^{\otimes n}$;

2. For every $(a, b) \in E$, apply a control-Z gate on qubits a and b ; the order can be arbitrary.

p

B. Entanglement Criteria

Entanglement of general mixed states was discussed by Werner in 1989 [20]. Since then, many entanglement criteria were proposed; among them the widely used ones

include the partial transpose criterion [12, 21, 22] and the symmetric extension criterion [23]. Entanglement of a many-body system can also be examined via its subsystems; that is, the subsystems are all entangled, then the whole system must be also entangled.

To be more concrete, consider a 4-qubit subsystem $\rho_{A,B,C,D}$ in a n qubit system. Suppose that we perform two local operations O_A and O_D on qubit A and D respectively, and then obtain the reduced density matrix of qubit B and C by tracing out qubit A and D . The reduced density matrix for qubits B and C reads

$$\rho'_{B,C} = \text{tr}_{A,D} \left(\frac{O_A O_D \rho_{A,B,C,D} O_D^\dagger O_A^\dagger}{\text{tr} \left(O_A O_D \rho_{A,B,C,D} O_D^\dagger O_A^\dagger \right)} \right). \quad (4)$$

The entanglement of $\rho'_{B,C}$ can be determined by using entanglement monotones such as negativity and concurrence, which, in the 2 qubit case, has non-zero values if and only if the system is entangled [12, 22]. If $\rho'_{B,C}$ is entangled, we can conclude that in the original system, there could not exist a separation with qubit B and C on different sides. In other words, if the original system is biseparable, the qubit B and C must be on the same side. Otherwise, we will be able to create entanglement between the two separable parties with only local operations, which is not possible [12].

For an n qubit system $\{q_1, q_2, \dots, q_n\}$, if we can show that among the n qubit pairs $(q_1, q_2), \dots, (q_{n-1}, q_n), (q_n, q_1)$, $n - 1$ of them must be on the same side in a separation, then we may conclude that there is no possible separation, and that the system is genuinely n -partite entangled. The (minimal) number of circuit configurations needed in this approach is $3^4 (n - 1)$, which grows linear with respect to n . This method is far more efficient compared to a full n -qubit tomography, which requires exponential number of configurations.

III. GRAPH STATES ON IBMQX5

ibmqx5 is a 16-qubit superconducting quantum processor. It allows independent single qubit operations with fidelity $> 99\%$ and control operations with fidelity $95 - 97\%$ [24] marked as the edges in the connectivity map (see Fig.1). That is, CNOT operations with qubit a as the control qubit and b as the target is allowed if and only if $a \rightarrow b$ is an edge in the map.

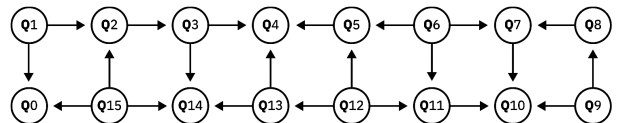


FIG. 1: Connectivity map of *ibmqx5* [24]

In our experiment, as shown in Fig. 2, the following three graph states are employed. The first state is a 8 qubit graph state involving qubits $q_5 - q_{12}$ that corresponds to a ring of length 8; the second one is a 10 qubit state involving qubits $q_4 - q_{13}$ corresponding to a ring of length 10; the third one involves qubits $q_3 - q_{14}$ and correspond to a ring of length 12.

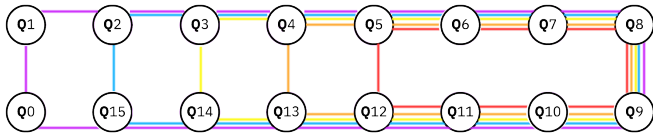


FIG. 2: Graph states employed in this experiment. Colored lines illustrate the graph of the 8 qubit graph state(in red), 10 qubit graph state(orange), 12 qubit graph state(yellow), 14 qubit state(blue) and 16 qubit graph state(purple).

We employ these particular graph states based on the following considerations. First, these states are genuinely entangled and will remain entangled after tracing out a large number of qubits. Second, research has shown that 1-D cluster states are robust against decoherence, meaning that it would be more likely to find entanglement in a rather large graph state close to a 1-D chain, compared to GHZ states and 2-D graph states [25]. At last, even rings are two-edge-colorable; as a result, on the 16-qubit *ibmqx5*, these “even-ring” states could be prepared using low-depth circuits. (See Fig. 3)

To prepare the desired graph state, we start from the circuit implied by the definition of graph states(see Fig. 3(a)). The control-Z gates are implemented using a CNOT gate and two Hadamard gates. We then optimize this circuit by adjusting the order of commuting gates and removing redundant Hadamard gates(see Fig. 3(b)). The circuit that we implemented are shown in Fig. 4(a)-Fig. 4(d).

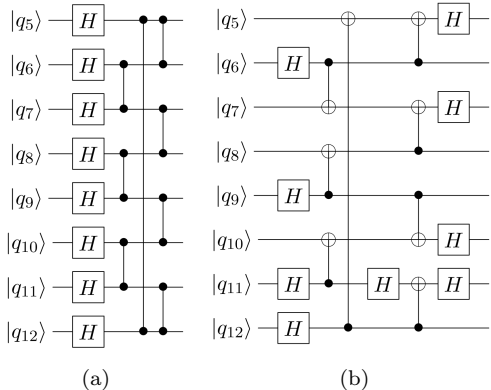


FIG. 3: (a) The quantum circuit for preparing a 8-qubit graph state implied by the definition of graph states; (b) The optimized circuit that suits *ibmqx5*'s connectivity.

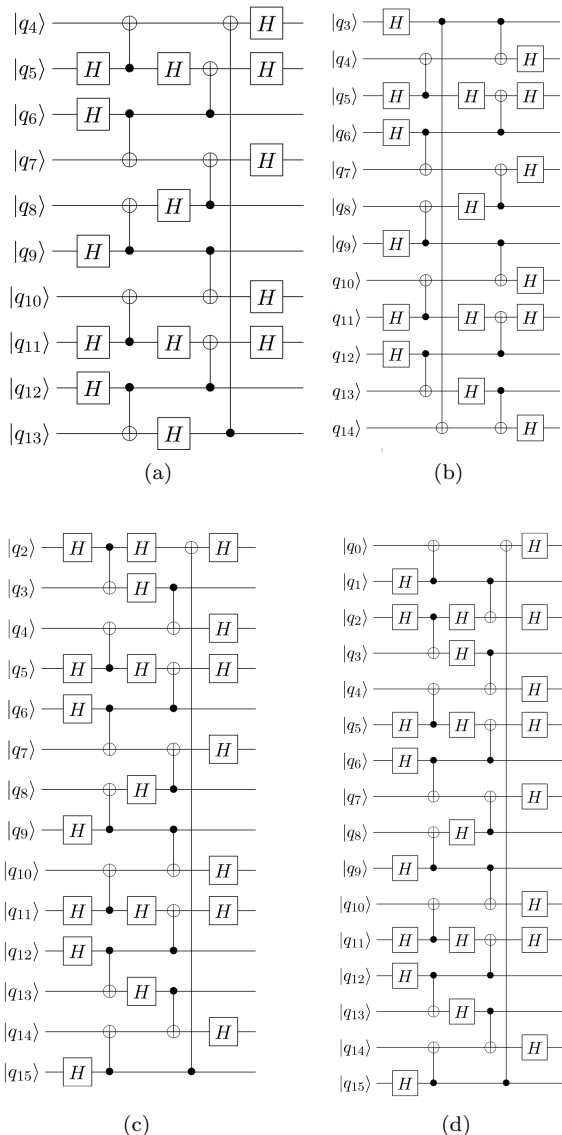


FIG. 4: The quantum circuit implemented on *ibmqx5* for the preparation of (a) 10 qubit graph state; (b) 12 qubit graph state; (c) 14 qubit graph state; (d) 16 qubit graph state.

IV. MAIN RESULTS

For each n -qubit ring state, n partial tomographies are performed for every subsystem with 4 qubits that forms a chain in the ring. E.g., for the 8-qubit graph state, the 8 subsystems are (q_5, q_6, q_7, q_8) , (q_6, q_7, q_8, q_9) , ..., (q_{12}, q_5, q_6, q_7) . For every state, $3^4 n$ experimental configurations are used; 2048 measurements are taken under each configuration. The n 4-qubit reduced density matrices are obtained using the maximum likelihood method proposed by J.Smolin et. al [26].

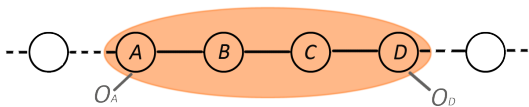


FIG. 5: A four-qubit subsystem that forms a chain

Due to Eq. (3), for a ring graph state, each 4-qubit density matrix of neighbouring four qubits, as illustrated in Fig 5 is given by

$$\rho_{A,B,C,D} = \frac{1}{4}(I + Z_A X_B Z_C)(I + Z_B X_C Z_D). \quad (5)$$

Then, for each 4-qubit density matrix, we apply the local operations $O_A = \frac{Z_A + I}{2}$ and $O_D = \frac{Z_D + I}{2}$ and calculate the negativity of the resulting 2-qubit subsystem. For instance, we may choose (q_5, q_6, q_7, q_8) as our subsystem; after applying O_A and O_D to q_5 and q_8 respectively, we will trace out q_5 and q_8 , and measure the negativity of the remaining subsystem, (q_6, q_7) . We choose $O_A = \frac{Z_A + I}{2}$ and $O_D = \frac{Z_D + I}{2}$ for the following reason. If ρ is graph state, and the 4-qubit subsystem corresponds to 4 vertices that form a chain in the graph, then the resulting 2-qubit state is a maximally entangled state

$$|\phi\rangle = \frac{1}{\sqrt{2}}(|0\rangle|+\rangle + |1\rangle|-\rangle). \quad (6)$$

Therefore, for a state close to this graph state, we should expect the resulting 2-qubit state to have a negativity significantly greater than zero. The results are plotted in Fig.6, Fig.7 and Fig.8.

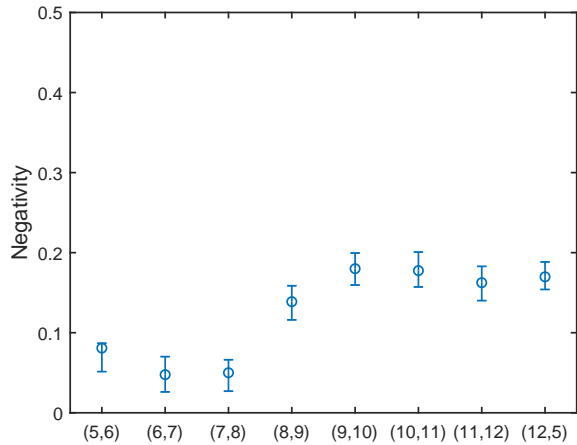


FIG. 6: The result of the 8 qubit graph state. The negativity of the 8 final 2-qubit states are plotted. (i, j) stands for the final 2-qubit system of (q_i, q_j) . For instance, entry (6, 7) is obtained by performing operations on $\rho_{q_5, q_6, q_7, q_8}$ and calculating the negativity of ρ'_{q_6, q_7} . 95% confidence intervals are estimated using bootstrapping techniques.

For the 8-qubit graph state, the measured negativities are all significantly greater than 0. For the 10-qubit

graph state, 9 out of 10 measured negativities are significantly greater than 0. Based on our argument in Sec. II B, both the 8-qubit state and 10-qubit state are genuinely entangled.

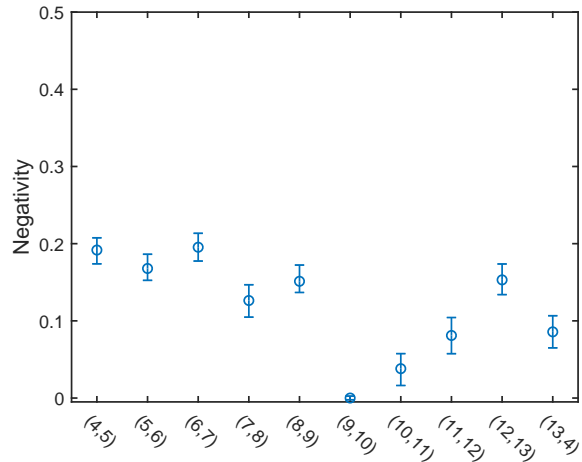


FIG. 7: The result of the 10 qubit graph state. The negativity of the 10 final 2-qubit states are plotted. 95% confidence intervals are estimated using bootstrapping techniques.

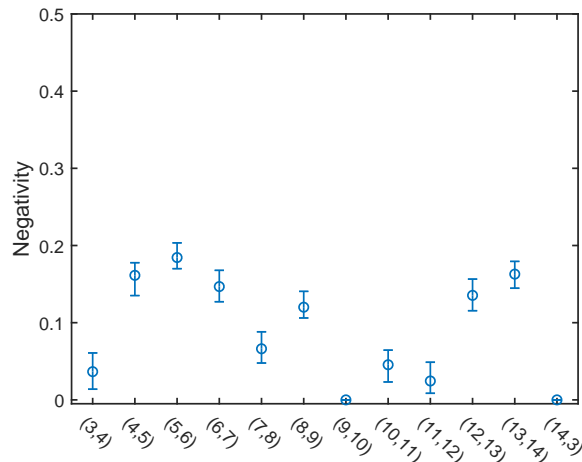


FIG. 8: The result of the 12 qubit graph state. The negativity of the 12 final 2-qubit states are plotted. 95% confidence intervals are estimated using bootstrapping techniques.

In the 12 qubit case, as shown in Fig. 8, 10 out of 12 measured negativities are significantly non-zero. The two zeros come from (q_9, q_{10}) and (q_{14}, q_3) pairs. Therefore, there is only one possible separation, namely $\{q_{10}, q_{11}, q_{12}, q_{13}, q_{14}\} | \{q_3, q_4, q_5, q_6, q_7, q_8, q_9\}$. Should this be true, the reduced density matrix of qubits q_8, q_9, q_{10}, q_{11} should also be separable with the separation $\{q_8, q_9\} | \{q_{10}, q_{11}\}$. In that case, its partial transpose with respect to qubit q_8 and q_9 must be positive. However, with respect to this partial transpose,

$\rho_{q8,q9,q10,q11}$ has negativity 0.0391 ± 0.0039 (standard deviation estimated via bootstrapping). Therefore, this possibility is ruled out with very high confidence. We can now conclude that the 12 qubit graph state is genuinely 12-partite entangled.

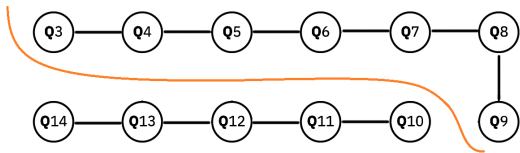


FIG. 9: The only possible separation based on the measured results in Fig. 8.

In the 14 qubit case, as shown in Fig. 10, 12 out of 14 measured negativites are significantly greater than 0. Here, we may apply the same trick again. The only possible separation is $\{q2, q3, q4, q5, q6, q7, q8, q9, q12, q13, q14\} | \{q10, q11\}$. In this case, subsystem $\{q8, q9, q10, q11\}$ should have zero negativity with respect to the partial transpose on $q8$ and $q9$. However, the measured negativity is 0.0698 ± 0.0048 (standard deviation estimated via bootstrapping). Hence, this possibility is ruled out with very high confidence. We may conclude that this state is genuinely fourteen-partite entangled.

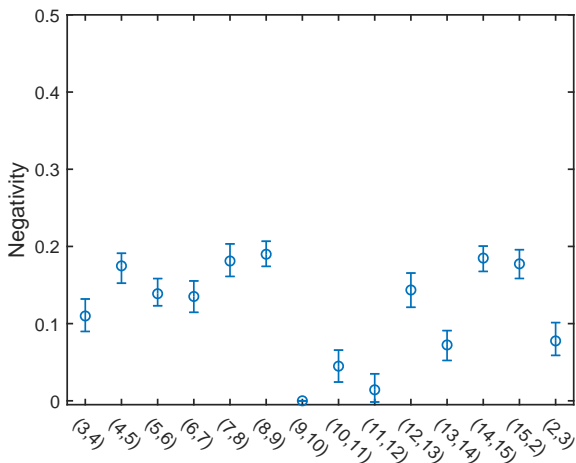


FIG. 10: The result of the 14 qubit graph state. The negativity of the 14 final 2-qubit states are plotted. 95% confidence intervals are estimated using bootstrapping techniques.

In the 16 qubit case, as shown in Fig. 11, 15 out of 16 measured negativites are significantly greater than 0. As argued in Sec. IIB, this means that this state is genuinely sixteen-partite entangled, thereby showing that all 16 qubits in *ibmqx5* are fully entangled.

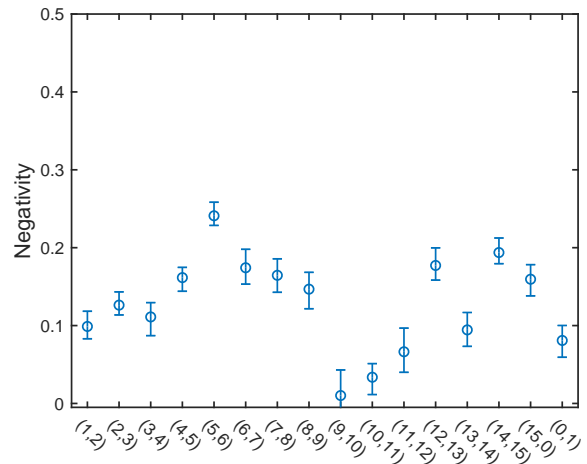


FIG. 11: The result of the 16 qubit graph state. The negativity of the 16 final 2-qubit states are plotted. 95% confidence intervals are estimated using bootstrapping techniques.

V. CONCLUSION AND DISCUSSION

We have prepared graph states of 8, 10, 12, 14 and 16 qubits on the 16-qubit *ibmqx5* processor and demonstrated that these graph states have genuine entanglement. In particular, we have realized full sixteen-partite entanglement using all 16 qubits. In our approach of detecting genuine entanglement, we only have to measure the reduced density matrix of up to 4 qubits, and the size of reduced density matrix does not scale with the total qubit number, i.e. our method is efficient and scalable. In our experiments, graph states do not have high fidelity because of the large number of qubits, e.g. the fidelity of the 12-qubit graph state is lower than 0.44. (This upperbound is obtained by computing the fidelity between each 4-qubit subsystem and the theoretical result and taking the minimum.) However, the negativity of 4-qubit reduced density matrix decays gently with respect to the qubit number, which implies that the error per qubit weakly depends on the qubit number. It is a strong evidence that *ibmqx5* is capable of generating highly entangled states and demonstrates the computer's quantumness. In computational tasks such as one-way quantum computing, graph state with decaying fidelity is acceptable, and the computing is fault-tolerant as long as the error per qubit is lower than a threshold [27, 28]. Because the negativity does not decay significantly, it is reasonable to conjecture that genuine entanglement of even more qubits may be detected on this device or even larger devices with similar performances.

The largest superconducting-qubit genuine entanglement reported in literature was 10-qubit GHZ state [15]. Our results also exceeds the largest genuinely entangled state in the ion trap systems, which is 14-qubit GHZ state [17]. Therefore, here we set a new record of the qubit number in multipartite entanglement in both the super-

conducting circuits and the trapped ions systems. It is noteworthy that our experiments are performed through cloud-based access to the quantum device, and are based on standardized universal quantum gate operations.

Acknowledgments

We gratefully acknowledge the IBM-Q team for providing us with access to their 16-qubit platform. The views

expressed are those of the authors and do not reflect the official policy or position of IBM or the IBM Quantum Experience team. Y.L. is supported by NSAF (Grant No. U1730449). Z.-Q.Y. is supported by the National Natural Science Foundation of China Grant 61771278, 11574176 and 11474177. B.Z. is supported by NSERC and CIFAR.

-
- [1] M. A. Nielsen and I. Chuang, *Quantum computation and quantum information* (2002).
- [2] N. Friis, O. Marty, C. Maier, C. Hempel, M. Holzäpfel, P. Jurcevic, M. Plenio, M. Huber, C. Roos, R. Blatt, et al., ArXiv e-prints (2017), 1711.11092.
- [3] *Ibm q experience*, <https://quantumexperience.ng.bluemix.net/qx/devices>, accessed: 2017-12-27.
- [4] J. Preskill, arXiv preprint arXiv:1203.5813 (2012).
- [5] D. Alsina and J. I. Latorre, *Physical Review A* **94**, 012314 (2016).
- [6] S. J. Devitt, *Physical Review A* **94**, 032329 (2016).
- [7] M. Berta, S. Wehner, and M. M. Wilde, *New Journal of Physics* **18**, 073004 (2016).
- [8] R. P. Rundle, P. W. Mills, T. Tilma, J. H. Samson, and M. J. Everitt, *Phys. Rev. A* **96**, 022117 (2017).
- [9] E. Huffman and A. Mizel, *Phys. Rev. A* **95**, 032131 (2017).
- [10] M. Hebenstreit, D. Alsina, J. I. Latorre, and B. Kraus, *Phys. Rev. A* **95**, 052339 (2017).
- [11] D. Ferrari and M. Amoretti, ArXiv e-prints (2018), 1801.02363.
- [12] R. Horodecki, P. Horodecki, M. Horodecki, and K. Horodecki, *Reviews of modern physics* **81**, 865 (2009).
- [13] H. J. Briegel and R. Raussendorf, *Physical Review Letters* **86**, 910 (2001).
- [14] R. Raussendorf and H. J. Briegel, *Physical Review Letters* **86**, 5188 (2001).
- [15] C. Song, K. Xu, W. Liu, C.-p. Yang, S.-B. Zheng, H. Deng, Q. Xie, K. Huang, Q. Guo, L. Zhang, et al., *Phys. Rev. Lett.* **119**, 180511 (2017).
- [16] R. Raussendorf and J. Harrington, *Phys. Rev. Lett.* **98**, 190504 (2007), URL <https://link.aps.org/doi/10.1103/PhysRevLett.98.190504>.
- [17] T. Monz, P. Schindler, J. T. Barreiro, M. Chwalla, D. Nigg, W. A. Coish, M. Harlander, W. Hänsel, M. Hennrich, and R. Blatt, *Phys. Rev. Lett.* **106**, 130506 (2011), URL <https://link.aps.org/doi/10.1103/PhysRevLett.106.130506>.
- [18] M. Hein, J. Eisert, and H. J. Briegel, *Physical Review A* **69**, 062311 (2004).
- [19] M. Hein, W. Dür, J. Eisert, R. Raussendorf, M. Van den Nest, and H. J. Briegel (2006), quant-ph/0602096.
- [20] R. F. Werner, *Physical Review A* **40**, 4277 (1989).
- [21] A. Peres, *Physical Review Letters* **77**, 1413 (1996).
- [22] M. Horodecki, P. Horodecki, and R. Horodecki, *Physics Letters A* **223**, 1 (1996), quant-ph/9605038.
- [23] A. C. Doherty, P. A. Parrilo, and F. M. Spedalieri, *Physical Review Letters* **88**, 187904 (2002).
- [24] *The ibm q experience ibmqx5 backend*, <https://github.com/QISKit/ibmqx-backend-information/tree/master/backends/ibmqx5>, accessed: 2017-12-27.
- [25] M. Hein, W. Dür, and H.-J. Briegel, *Phys. Rev. A* **71**, 032350 (2005).
- [26] J. A. Smolin, J. M. Gambetta, and G. Smith, *Phys. Rev. Lett.* **108**, 070502 (2012).
- [27] M. A. Nielsen and C. M. Dawson, *Phys. Rev. A* **71**, 042323 (2005), URL <https://link.aps.org/doi/10.1103/PhysRevA.71.042323>.
- [28] R. Raussendorf, J. Harrington, and K. Goyal, *Annals of Physics* **321**, 2242 (2006), ISSN 0003-4916, URL <http://www.sciencedirect.com/science/article/pii/S0003491606000236>.